Structural Engineering and Mechanics, *Vol. 63, No. 1 (2017) 103-113*
DOI: https://doi.org/10.12989/sem.2017.63.1.103

Eigenfrequencies of simply supported taper plates with cut-outs

Kanak Kalita* and Salil Haldar

Department of Aerospace Engineering and Applied Mechanics, Indian Institute of Engineering Science and Technology, Shibpur, Howrah - 711103, West Bengal, India

(Received July 14, 2016, Revised June 3, 2017, Accepted June 5, 2017)

Abstract. Free vibration analysis of plates is necessary for the field of structural engineering because of its wide applications in practical life. Free vibration of plates is largely dependent on its thickness, aspect ratios, and boundary conditions. Here we investigate the natural frequencies of simply supported tapered isotropic rectangular plates with internal cutouts using a nine node isoparametric element. The effect of rotary inertia on Eigenfrequencies was demonstrated by calculating with- and without rotary inertia. We found that rotary inertia has a significant effect on thick plates, while rotary inertia term can be ignored in thin plates. Based on comparison with literature data, we propose that the present formulation is capable of yielding highly accurate results. Internal cutouts at various positions in tapered rectangular simply supported plates were also studied. Novel data are also reported for skew taper plates.

Keywords: finite element method; FSDT; rectangular plate; taper; rotary inertia; free vibration

1. Introduction

Dynamic analysis of plate structures has received a lot of attention due to their endless applications. A number of plate theories have been put forward by various researchers. Among them, classical plate theory (CPT) introduced by Kirchhoff (Kirchhoff 1850) (Kirchhoff 1850) is most well-known. It is based on the assumption that straight lines normal to the undeformed midplane remain straight and normal to the deformed midplane and hence transverse shear are zero. However, for analyzing the problems of the thick plate as well as a thin plate with holes, the classical theory is not sufficient. (Ozdemir and Ayvaz 2014). The effect of transverse shear is necessary for these types of problems. Therefore, some corrections in the CPT are essential. In this regard, the first order shear deformation theory (FSDT) and higher order shear deformation theory (HSDT) are important. FSDT is an extension of CPT that takes into account shear deformations through-the-thickness of a plate. FSDT assumes that though the normal to the undeformed midplane remain straight, it need not be necessarily normal to the midplane after deformation. Mindlin's theory (Mindlin 1951) assumes that there is a linear variation of displacement across the plate thickness. Reissner proposed a similar theory that assumes the bending stress to be linear while the shear stress is quadratic through the thickness of the plate (Reissner 1944) (Reissner 1945). FSDT is also simpler in the regard that it has three coupled PDEs whereas CPT leads to fourth order PDE which usually cannot be decoupled (Dalir and Shooshtari 2015). The higher order shear deformation theory developed by Reddy (Reddy 1984) takes into account transverse shear strains which vary parabolically through the thickness. Hence there is no need to use shear correction coefficients in the computing of shear stresses.

The analytical solutions of the plates are available only for its regular shapes having simple boundary conditions. In this context, different numerical methods such as finite difference, finite strip, and finite element methods are used, depending on the suitability of the problems. The study of Eigenfrequencies of rectangular plates has a long and established history. A number of literature are available on free vibration of rectangular plates of uniform thickness. Liew *et al.* (Liew *et al.* 1995) have compiled a list of several works on free vibration of plates. They have systematically classified the contemporary literature on free vibration and focuses on works based on Mindlin theory and modified Mindlin theory.

Though the literature available on free vibration of rectangular plates of uniform thickness is vast, work done considering taper plates is limited. Taper plates find a lot of application in marine and aero structures like turbine discs, aircraft wings etc. An almost exhaustive list of works on free vibration of rectangular taper plate in one direction is provided here. This survey is limited to available literature in English only. Mlzusawa (Mlzusawa 1993) used the spline strip method to calculate the Eigenfrequencies of rectangular Mindlin plates linearly varying in thickness. Free vibration behavior of isotropic linearly varying rectangular plates was studied by Aksu and Al-Kaabi (Aksu and Al-Kaabi 1987) using the finite difference method. They considered the effect of transverse shear deformation and rotary inertia while calculating the natural frequencies. Bert and Malik (Bert and Malik 1996) used differential quadrature method to find out the natural frequencies of tapered rectangular plates having two opposite edges simply supported. Cheung and Zhou (Cheung and Zhou 1999a) considered the free vibrations of a wide range of non-

*Corresponding author
E-mail: kanakkalita02@gmail.com

ISSN: 1225-4568 (Print), 1598-6217 (Online)

uniform rectangular plates in one or two directions. In the same year Cheung and Zhou (Cheung and Ding 1999b) carried out a study on the free vibrations of a wide range of tapered rectangular plates with an arbitrary number of intermediate line supports in one or two directions. The thickness of the plate is varied continuously and was proportional to a power function $x^s y^t$. The Eigen frequency equation of the plate was derived by the Rayleigh-Ritz approach. Zhou (Zhou 2002) studied the free vibrations of point-supported rectangular plates with variable thickness using the Rayleigh-Ritz method. Cheung and Zhou (Cheung and Zhou 2003) investigated the free vibrations of rectangular Mindlin plates with variable thickness in one or two directions. The thickness variation of the plate was continuous and represented by a power function of the rectangular co-ordinates. A sub-parametric shear deformable element with sixteen nodes and thirty-six degrees of freedom based on first-order shear deformation theory (FSDT) was used by Manna (Manna 2006) for free vibration analysis of isotropic plates with a linearly varying thickness in one direction. Manna (Manna 2011) presented the first six modes of free vibration for isotropic rectangular plates linearly varying in one direction. He used a higher order triangular element to analyze the problem for different taper ratio, aspect ratio, and different boundary conditions. Bhat *et al*. (Bhat *et al*. 1990) compared natural frequencies of transverse vibration of thin non-uniform rectangular plates using the Rayleigh-Ritz method, optimized Kantorovich method and the finite element method. Basic displacement functions in plate elements which take thickness variation and Eigenfrequencies of the plates into account has been used to calculate shape functions of tapered Mindlin plates for the free vibration analysis by Pachenari and Attarnejad (Pachenari and Attarnejad 2014) (Pachenari and Attarnejad 2014). Rajasekaran and Wilson (Rajasekaran and Wilson 2013) has used the finite difference method to predict the natural frequencies of rectangular plates of variable thickness.

Cutouts in plates are often provided for the functional or esthetic purpose. For example various shaped cutouts are provided as manhole of pressure vessels, window and door of vehicles or aircrafts, entry to submarine hull etc. However, these cutouts change the mass and rigidity of a plate and in turn alter the natural frequencies. Hence from a design perspective, their effect must be accurately calculated. In past several numerical solutions have been reported for rectangular plates/shells with cutouts having a uniform thickness (Lee and Chen 2010) (Sahoo 2015) (Saeedi *et al*. 2012) (Lee *et al*. 2007). Larrondo *et al*. (Larrondo *et al*. 2001) illustrated the effect of the cutout on taper plates by using the Rayleigh-Ritz variational approach. Sahoo (Sahoo 2015) used an eight node quadrilateral element to study the effect of position and size of cutout on natural frequency of shells. Saeedi *et al*. (Saeedi *et al*. 2012) used the Rayleigh-Ritz method to study the effect of multiple circular cutouts in a circular plate. They reported that the cutouts cause both mass and stiffness reduction, thereby effecting the natural frequencies. In a recent research, Kalita and Haldar (Kalita and Haldar 2016) reported the effect of a central rectangular cutout in plates. They observed that with increase in cutout size the frequency parameters increase, due to reduction in mass of the plate.

In the present work, a nine node isoparametric element is used to calculate the Eigenfrequencies of rectangular plates with a taper in one direction. A generalized finite element computer code is written using first order shear deformation theory because it is simple to implement and gives better results than the CPT since the generalized displacement field not only requires any derivative but also includes transverse shear strains. Also, the computational cost using the FSDT is cheaper than that using the HSDT. Two mass lumping schemes are applied in this work to compute the Eigenfrequencies by considering the effect of rotary inertia and without taking into account rotary inertia. Though the utility of considering rotary inertia in thick and moderately thick plates has been highlighted by some researchers, a revisit to this issue is made here since such comparison is not available for taper plates. Also, the existing literature lacks a thorough comparison of natural frequencies calculated with and without considering rotary inertia. A simple comparison regarding percentage variation in computed frequencies is presented here for rectangular taper plates. To the best of author's knowledge, this has not been done for taper thickness plates. Several numerical examples are solved for rectangular taper plates with rectangular cutouts at various positions. Sets of first time reported Eigen frequency data for rectangular skew taper plate with and without central cutout are also provided here for future reference.

2. Finite element formulation

In the current formulation, FEM has been used for free vibration analysis of the plate. The midplane is assumed to be the reference plane. This was done using the theory of Mindlin plate where it is assumed that the normal to the midplane of the plate remains straight but not necessarily normal to the deformed mid-surface. The first order shear deformation theory (FSDT) assumes the displacement through the thickness of the plate to be linear. However, there is no change in thickness of the plate after deformation. Further, the normal stress throughout the thickness is ignored; a hypothesis which is also called the plane stress state. Though the shear strain is not neglected in this theory, the assumption that it is constant over the entire thickness of the plate is not true. Across the thickness of the plate, the shear stress is known to be parabolic. Hence a shear correction factor is applied. This ensures that the theory predicts the correct amount of internal energy. In the past, this formulation has been used by the author for analysis of shell (Majumdar, Manna and Haldar 2010) and composite plates (Pandit, Haldar and Mukhopadhyay 2007). This formulation has been shown to work sufficiently well for thick plates (Kalita and Haldar 2015) and even plates with central openings (Kalita and Haldar 2016). A more detailed analysis of vibration of plates can be found in (Algazin 2010) (Chakraverty 2008).

A nine-node isoparametric element is used in the current

finite element formulation. One of the main advantages of the element is that any form of plate can be well managed with an elegant mapping technique that can be defined as

$$x = \sum_{r=1}^{9} N_r x_r \ and \ y = \sum_{r=1}^{9} N_r y_r \tag{1}$$

Thus by using this simple mapping technique the coordinates at any place within the element (x, y) are expressed as the summation of the product of the Lagrange interpolation function (N_r) and the coordinates of the rth nodal point (x_r, y_r). Considering the bending rotations as independent field variables (since they are not derivatives of w), the effect of shear deformation may be incorporated as

$$\begin{Bmatrix} \phi_x \\ \phi_y \end{Bmatrix} = \begin{Bmatrix} \theta_x - \dfrac{\partial w}{\partial x} \\ \theta_y - \dfrac{\partial w}{\partial y} \end{Bmatrix}$$

Since this is an isoparametric formulation the same interpolation functions used for element geometry have been used to describe the displacement field at any point within the element in terms of nodal variables as

$$w = \sum_{r=1}^{9} N_r w_r, \ \theta_x = \sum_{r=1}^{9} N_r \theta_{xr} \ \text{and} \ \theta_y = \sum_{r=1}^{9} N_r \theta_{yr} \tag{2}$$

The stresses and strains of any continuous elastic material are connected by a linear relationship that is mathematically similar to Hooke's law and may be expressed as

$$\{\sigma\} = [D]\{\varepsilon\} \tag{3}$$

Where,

$$\{\sigma\} = [M_x \quad M_y \quad M_{xy} \quad Q_x \quad Q_y] \tag{4}$$

$$\{\varepsilon\} = \begin{Bmatrix} -\partial\theta_x/\partial x \\ -\partial\theta_y/\partial y \\ -\partial\theta_x/\partial y - \partial\theta_y/\partial x \\ \partial w/\partial x - \theta_x \\ \partial w/\partial y - \theta_y \end{Bmatrix} \tag{5}$$

Using Eqs. (2) and (5)

$$\begin{aligned} \frac{-\partial\theta_x}{\partial x} &= -\left(\frac{\partial N_r}{\partial x}\right)\theta_{xr} \,;\, \frac{-\partial\theta_y}{\partial y} \\ &= -\left(\frac{\partial N_r}{\partial y}\right)\theta_{yr} \,;\, \frac{-\partial\theta_x}{\partial y} + \frac{-\partial\theta_y}{\partial x} \\ &= -\left(\frac{\partial N_r}{\partial y}\right)\theta_{xr} - \left(\frac{\partial N_r}{\partial x}\right)\theta_{yr} \,;\, \frac{\partial w}{\partial x} \\ &\quad - \theta_x \\ &= -\left(\frac{\partial N_r}{\partial x}\right) w_r - (N_r)\theta_{xr} \,;\, \frac{\partial w}{\partial y} - \theta_y \\ &= -\left(\frac{\partial N_r}{\partial y}\right) w_r - (N_r)\theta_{yr} \end{aligned} \tag{6}$$

$$[D] = \begin{bmatrix} D_{11} & D_{12} & 0 & 0 & 0 \\ D_{21} & D_{22} & 0 & 0 & 0 \\ 0 & 0 & D_{33} & 0 & 0 \\ 0 & 0 & 0 & D_{44} & 0 \\ 0 & 0 & 0 & 0 & D_{55} \end{bmatrix}$$

Where,

$$D_{11} = D_{22} = \frac{E}{1-\nu^2}; D_{12} = D_{21} = \nu D_{11}; D_{33} = \frac{E}{2(1+\nu)}$$

$$D_{44} = D_{55} = \frac{Ehk}{2(1+\nu)}$$

Here, k is the shear correction factor.

From Eqs. (2) and (5) the strain vector may be expressed as

$$\{\varepsilon\} = \sum_{r=1}^{9} [B]_r \{\delta_r\}_e \tag{7}$$

[B] is the strain-displacement matrix containing interpolation functions and their derivatives.

Using the virtual work method, the stiffness may be expressed as

$$[K] = h \int_{-1}^{+1} \int_{-1}^{+1} [B]^T [D][B]|J| d\xi d\eta \tag{8}$$

Where $|J|$ is the determinant of the Jacobian matrix.

Similarly, the consistent mass matrix may be expressed as

$$[M] = \rho h \int_{-1}^{1} \int_{-1}^{1} \left([N_w]^T [N_w] + \frac{h^2}{12} [N_{\theta x}]^T [N_{\theta x}] + \frac{h^2}{12} [N_{\theta y}]^T [N_{\theta y}] \right) |J| d\xi d\eta \tag{9}$$

The global stiffness matrix [K_0] and global mass matrix [M_0] are calculated by assembling individual stiffness matrix and the individual mass matrices of all the elements. Using equation of motion, we get

$$[K_0] = \omega^2 [M_0] \tag{10}$$

The taper ratio as shown in Fig. 1 is defined as $h_1 = h(1 + \delta_o)$. The calculated frequencies are presented in non-dimensional form $\lambda = \omega a^2 \sqrt{\rho h / D}$ where $D = \frac{Eh^3}{12(1-\nu^2)}$.

3. Convergence and validation

To demonstrate the accuracy and convergence of the current computer code developed based on the finite element formulation in section 2 some numerical examples from existing literature is solved and compared. Mesh division is designated as (m×n) if the plate is divided into m equal divisions along the x-direction and n equal divisions along the y-direction. Herein, two different types of mass lumping schemes are considered -LSWRI (with rotary inertia) and other is LSWORI (without rotary inertia). The convergence study and comparison tests for a clamped simply supported rectangular plate with a linearly varying thickness in the x-direction are carried out. The boundary conditions are:

Table 1 Convergence study of the dimensionless frequencies $\lambda = \omega a^2\sqrt{\rho h/D}$ for CSCS taper rectangular plate

δ_o	Source	Modes					
		1	2	3	4	5	6
0.2	LSWRI(10*10)	31.7611	60.0047	75.9792	103.5761	111.8602	141.3978
	LSWRI(12*12)	31.7596	60.0036	75.9655	103.5803	111.8335	141.2931
	LSWRI(16*16)	31.7578	60.0022	75.955	103.582	111.8157	141.2267
	LSWRI(18*18)	31.7573	60.0018	75.9526	103.5819	111.8133	141.2137
	LSWORI(10*10)	31.7646	60.0201	76.0004	103.6198	111.9159	141.4747
	LSWORI(12*12)	31.7631	60.019	75.9866	103.624	111.8891	141.3697
	LSWORI(16*16)	31.7613	60.0176	75.9761	103.6256	111.8712	141.3031
	LSWORI(18*18)	31.7608	60.0171	75.9738	103.6255	111.8689	141.2900
	(Bert and Malik 1996)	31.7869	60.0876	76.1115	103.8624	112.0735	141.7216
	(Bhat *et al.* 1990)	31.7870	60.0877	76.1121	103.8630	112.7190	141.9000
	% error (1)	0.09	0.14	0.21	0.27	0.23	0.36
	% error (2)	0.09	0.14	0.21	0.27	0.80	0.48
0.4	LSWRI(10*10)	34.5089	65.1354	82.5188	112.5242	121.0865	153.5063
	LSWRI(12*12)	34.5031	65.1289	82.4941	112.5178	121.0503	153.3741
	LSWRI(16*16)	34.4971	65.1218	82.4723	112.5079	121.0232	153.2813
	LSWRI(18*18)	34.4954	65.1198	82.4669	112.5047	121.0178	153.2657
	LSWORI(10*10)	34.5134	65.1550	82.5460	112.5805	121.1568	153.6050
	LSWORI(12*12)	34.5076	65.1485	82.5213	112.574	121.1205	153.4722
	LSWORI(16*16)	34.5016	65.1414	82.4995	112.564	121.0933	153.3792
	LSWORI(18*18)	34.4999	65.1394	82.4941	112.5609	121.088	153.3635
	(Bert and Malik 1996)	34.5237	65.2136	82.6464	112.8339	121.3219	153.8701
	(Bhat *et al.* 1990)	34.5237	65.2138	82.6479	112.8360	122.0160	153.9780
	% error (1)	0.08	0.14	0.22	0.29	0.25	0.39
	% error (2)	0.08	0.14	0.22	0.29	0.82	0.46

Table 2 Dimensionless frequencies $\lambda = \omega a^2\sqrt{\rho h/D}$ for SSSS taper rectangular plate [h/a=0.001]

δ_o	a/b	Source	Modes					
			1	2	3	4	5	6
0.1	0.5	LSWRI(18*18)	12.9458	20.7193	33.6654	43.9587	51.7946	51.8124
		LSWORI(18*18)	12.9458	20.7194	33.6656	43.959	51.795	51.8129
	1	LSWRI(18*18)	20.7206	51.7836	51.7945	82.8764	103.5129	103.5853
		LSWORI(18*18)	20.7206	51.7837	51.7946	82.8767	103.5133	103.5858
	1.5	LSWRI(18*18)	33.6688	64.7476	103.5875	116.5169	134.6658	186.4708
		LSWORI(18*18)	33.6688	64.7477	103.5877	116.5172	134.6662	186.4715
	2	LSWRI(18*18)	51.7929	82.8821	134.6688	176.0971	207.157	207.1746
		LSWORI(18*18)	51.7929	82.8822	134.669	176.0974	207.1575	207.1751
0.25	0.5	LSWRI(18*18)	13.8327	22.1679	36.0016	46.7089	55.3753	55.5024
		LSWORI(18*18)	13.8328	22.168	36.0018	46.7093	55.3758	55.503
	1	LSWRI(18*18)	22.1744	55.3313	55.3948	88.6708	110.3289	110.7484
		LSWORI(18*18)	22.1744	55.3315	55.3949	88.6711	110.3295	110.749
	1.5	LSWRI(18*18)	36.0201	69.2699	110.7771	124.4991	144.0441	199.5095
		LSWORI(18*18)	36.0202	69.27	110.7773	124.4995	144.0445	199.5103
	2	LSWRI(18*18)	55.3839	88.6971	144.0375	188.3113	221.3492	221.5755
		LSWORI(18*18)	55.3839	88.6972	144.0377	188.3117	221.3498	221.5761

Table 2 Continued

δ_o	a/b	Source	Modes					
			1	2	3	4	5	6
0.5	0.5	LSWRI(18*18)	15.2543	24.5339	39.7909	50.7694	61.1621	61.5699
		LSWORI(18*18)	15.2543	24.534	39.7912	50.7699	61.1629	61.5707
	1	LSWRI(18*18)	24.5569	61.0164	61.2438	98.1348	120.8479	122.3279
		LSWORI(18*18)	24.5569	61.0166	61.244	98.1353	120.8487	122.3287
	1.5	LSWRI(18*18)	39.8572	76.6507	122.4403	137.2908	159.3042	220.7991
		LSWORI(18*18)	39.8572	76.6508	122.4406	137.2912	159.3048	220.8002
	2	LSWRI(18*18)	61.2032	98.2272	159.2701	208.1138	244.0911	244.9712
		LSWORI(18*18)	61.2032	98.2274	159.2704	208.1143	244.0919	244.972
0.75	0.5	LSWRI(18*18)	16.6201	26.8511	43.4769	54.4014	66.7699	67.4747
		LSWORI(18*18)	16.6202	26.8513	43.4773	54.402	66.7709	67.4757
	1	LSWRI(18*18)	26.899	66.4801	66.9427	107.4038	130.5964	133.5521
		LSWORI(18*18)	26.899	66.4803	66.9429	107.4045	130.5973	133.5532
	1.5	LSWRI(18*18)	43.6125	83.8758	133.785	149.5843	174.1984	239.8768
		LSWORI(18*18)	43.6126	83.876	133.7855	149.5848	174.1992	239.8782
	2	LSWRI(18*18)	66.8583	107.5955	174.1255	227.3661	265.9469	267.7664
		LSWORI(18*18)	66.8584	107.5956	174.1259	227.3668	265.9479	267.7674

Simply supported condition (denoted by S):

$w = \theta_x = 0$, At boundary line parallel to x-axis

$w = \theta_y = 0$, At boundary line parallel to y-axis

Clamped condition (denoted by C):

$w = \theta_x = \theta_y = 0$

The first six natural frequencies are calculated for various taper ratio and compared with results reported by Bert and Malik (Bert and Malik 1996) calculated using differential quadrature method and Bhat *et al*. (Bhat *et al*. 1990) calculated using Rayleigh-Ritz method. Results for a moderately thick square plate having thickness ratio (h/a) 0.01 at taper ratio (δ_o) 0.2 and 0.4 is reported in Table 1. Poisson's ratio 0.3 is considered in all cases. Excellent convergence is seen at mesh size 18*18 and hence this mesh is used throughout the study for solid plates and mesh size of 20*20 is used for perforated plates. Comparative results for rectangular plates with existing literature is illustrated in Fig. 2. It can be seen that Eigenfrequencies calculated with rotary inertia are in better agreement with existing literature, since in (Bert and Malik 1996) and (Bhat *et al*. 1990) effect of rotary inertia was taken into account. The percentage error between the present solution i.e., LSWRI(18*18) and (Bert and Malik 1996) and (Bhat *et al*. 1990) are reported here as % error (1) and % error (2) respectively. % error is calculated as,

$$\% \text{ error} = \frac{\left(\omega_{Ref} - \omega_{LSWRI(18*18)}\right) \times 100}{\omega_{Ref}}$$

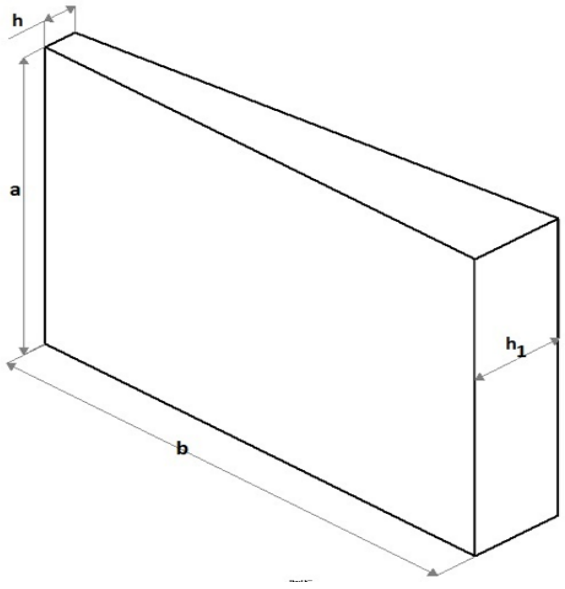

Fig. 1 Rectangular taper plate considered in the study

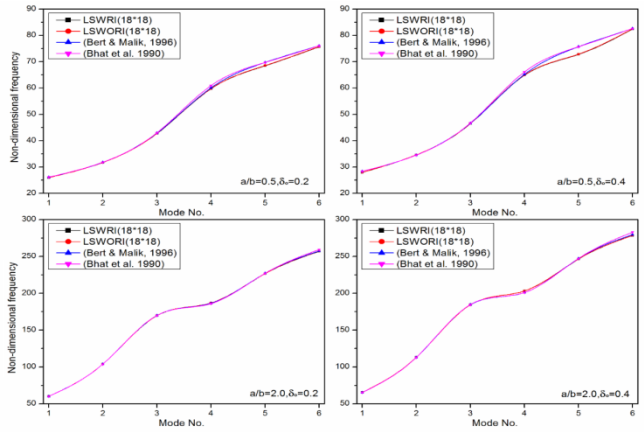

Fig. 2 Comparison of present results with literature

Table 3 Dimensionless frequencies $\lambda = \omega a^2\sqrt{\rho h/D}$ for SSSS taper rectangular plate [h/a=0.01]

δ_o	a/b	Source	Modes					
			1	2	3	4	5	6
0.1	0.5	LSWRI(18*18)	12.933	20.687	33.58	43.813	51.592	51.609
		LSWORI(18*18)	12.9363	20.6945	33.5994	43.8461	51.6378	51.6554
	1	LSWRI(18*18)	20.713	51.7337	51.7446	82.7476	103.3108	103.383
		LSWORI(18*18)	20.7149	51.7454	51.7563	82.7774	103.3573	103.4296
	1.5	LSWRI(18*18)	33.6601	64.7139	103.4987	116.4044	134.5166	186.1819
		LSWORI(18*18)	33.6623	64.7221	103.5196	116.4307	134.5517	186.2491
	2	LSWRI(18*18)	51.7812	82.8518	134.5864	175.9527	206.9572	206.9752
		LSWORI(18*18)	51.7841	82.8594	134.6061	175.9865	207.0039	207.0219
0.25	0.5	LSWRI(18*18)	13.8185	22.1301	35.8997	46.5376	55.1316	55.2563
		LSWORI(18*18)	13.8221	22.1392	35.9237	46.5772	55.1881	55.3133
		(Manna 2011)	13.817	22.127	35.895	46.531	55.119	55.248
	1	LSWRI(18*18)	22.1668	55.2745	55.3383	88.5197	110.0923	110.5101
		LSWORI(18*18)	22.1691	55.2887	55.3526	88.5564	110.1483	110.5671
		(Manna 2011)	22.164	55.266	55.332	88.509	110.07	110.49
	1.5	LSWRI(18*18)	36.0124	69.2342	110.6776	124.3713	143.8719	199.1685
		LSWORI(18*18)	36.0151	69.2442	110.7031	124.4034	143.915	199.2509
	2	LSWRI(18*18)	55.3738	88.6671	143.9475	188.1505	221.1216	221.3496
		LSWORI(18*18)	55.3774	88.6764	143.9717	188.192	221.1786	221.4069
		(Manna 2011)	55.368	88.656	143.93	188.13	221.07	221.33
0.5	0.5	LSWRI(18*18)	15.2377	24.4872	39.6607	50.5595	60.8453	61.2447
		LSWORI(18*18)	15.2424	24.4997	39.6933	50.6095	60.9215	61.3224
		(Manna 2011)	15.231	24.478	39.646	50.54	60.819	61.219
	1	LSWRI(18*18)	24.5515	60.9512	61.1798	97.9482	120.5585	122.0313
		LSWORI(18*18)	24.5547	60.9702	61.1993	97.9981	120.6313	122.1084
		(Manna 2011)	24.543	60.925	61.16	97.911	120.5	121.99
	1.5	LSWRI(18*18)	39.8544	76.6169	122.3311	137.1438	159.1025	220.3792
		LSWORI(18*18)	39.8581	76.6304	122.3658	137.1866	159.1611	220.4915
	2	LSWRI(18*18)	61.2012	98.2058	159.1784	207.9406	243.8298	244.7154
		LSWORI(18*18)	61.2062	98.2184	159.2111	207.9969	243.9059	244.7933
		(Manna 2011)	61.186	98.171	159.11	207.88	243.7	244.64
0.75	0.5	LSWRI(18*18)	16.6024	26.7958	43.3165	54.1559	66.3722	67.0619
		LSWORI(18*18)	16.6085	26.8122	43.3591	54.2163	66.4715	67.1637
	1	LSWRI(18*18)	26.8981	66.4098	66.8749	107.1822	130.2588	133.1974
		LSWORI(18*18)	26.9022	66.4343	66.9005	107.2479	130.3494	133.2982
	1.5	LSWRI(18*18)	43.6188	83.8503	133.6766	149.4258	173.9741	239.3902
		LSWORI(18*18)	43.6238	83.8681	133.7222	149.4807	174.0511	239.528
	2	LSWRI(18*18)	66.8708	107.5919	174.044	227.1966	265.6657	267.4954
		LSWORI(18*18)	66.8775	107.6086	174.0868	227.2706	265.7635	267.5979

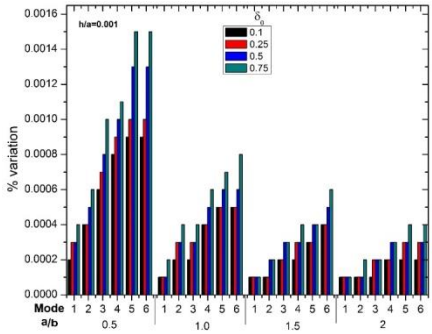

Fig. 3 Percent Variation of λ_i (calculated with- and without- rotary inertia)

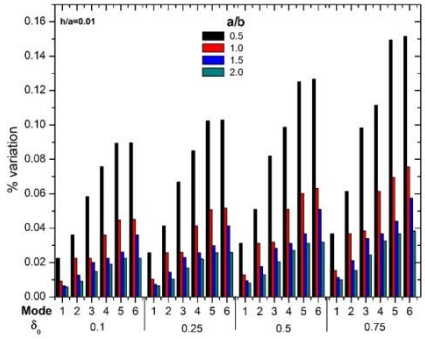

Fig. 4 Percent Variation of λ_i (calculated with- and without- rotary inertia)

Table 4 Dimensionless frequencies $\lambda = \omega a^2\sqrt{\rho h/D}$ for SSSS taper rectangular plate with internal cut-out at various positions

h/a	a/b	δ_o	Cut-out Position	Source	Modes					
					1	2	3	4	5	6
0.01	0.5	0.25	A	LSWRI(20*20)	12.9204	21.8955	36.1503	41.5426	53.692	53.9957
			B	LSWRI(20*20)	13.411	21.5075	35.3418	46.3303	54.1634	54.9354
			C	LSWRI(20*20)	13.4772	21.8147	36.0155	43.518	51.4432	54.3587
			D	LSWRI(20*20)	13.2916	21.5398	35.4072	44.8704	53.8226	55.1046
		0.5	A	LSWRI(20*20)	14.3271	24.2399	39.9466	45.9088	59.1225	59.7515
			B	LSWRI(20*20)	14.7881	23.7585	39.0963	51.3299	59.742	60.9983
			C	LSWRI(20*20)	14.9111	24.1992	39.8033	48.1091	56.8784	59.9132
			D	LSWRI(20*20)	14.8034	23.8054	39.1767	49.4063	59.4041	60.8658
	1	0.25	A	LSWRI(20*20)	21.4802	53.2155	53.2681	85.6137	106.9866	115.1128
			B	LSWRI(20*20)	21.6367	54.4271	54.8411	89.0104	107.5315	111.6359
			C	LSWRI(20*20)	21.7501	53.7993	54.3329	86.2071	107.147	112.392
			D	LSWRI(20*20)	21.8514	53.8177	54.2815	86.0073	107.6502	111.8546
		0.5	A	LSWRI(20*20)	23.8556	58.6243	58.8118	94.7765	117.6087	125.6932
			B	LSWRI(20*20)	23.9651	60.0972	60.6291	98.7376	118.0029	123.2848
			C	LSWRI(20*20)	24.1021	59.4404	59.9442	95.4741	117.6948	123.3777
			D	LSWRI(20*20)	24.2852	59.4151	59.9604	94.9953	118.6781	122.5826
0.1	0.5	0.25	A	LSWRI(20*20)	12.4926	20.836	33.6621	35.8599	48.2114	48.7667
			B	LSWRI(20*20)	12.957	20.4431	32.8084	42.4507	48.797	49.5813
			C	LSWRI(20*20)	13.066	20.8414	33.5205	37.708	46.0524	48.7631
			D	LSWRI(20*20)	12.7569	20.4744	32.7886	41.0025	48.2859	49.8452
		0.5	A	LSWRI(20*20)	13.7897	22.8715	36.5996	38.9952	52.1806	52.9747
			B	LSWRI(20*20)	14.2293	22.429	35.8694	46.3251	52.8747	54.0986
			C	LSWRI(20*20)	14.3874	22.9300	36.5028	40.942	50.0098	52.7940
			D	LSWRI(20*20)	14.1276	22.4076	35.7852	44.3532	52.3183	54.0617
	1	0.25	A	LSWRI(20*20)	20.5395	46.9178	46.9648	73.8243	89.4023	96.0873
			B	LSWRI(20*20)	20.5842	48.9368	49.5707	76.3959	88.7862	93.2125
			C	LSWRI(20*20)	20.7044	48.0943	49.1427	72.9255	88.6925	93.8727
			D	LSWRI(20*20)	20.7998	48.1471	49.035	72.6598	89.1871	93.5833
		0.5	A	LSWRI(20*20)	22.6423	50.7054	50.8597	79.5183	95.5416	101.8309
			B	LSWRI(20*20)	22.6431	53.1556	53.8000	82.4825	94.6439	99.9334
			C	LSWRI(20*20)	22.7506	52.1247	53.2929	78.5725	94.7078	100.0947
			D	LSWRI(20*20)	22.9266	52.207	53.1484	77.9594	95.6322	99.7636

4. Numerical results

4.1 Taper thickness rectangular plates

Simply supported isotropic rectangular plates having different thickness ratios, aspect ratios, and different boundary conditions have been considered in this study. The Poisson's ratio (ν) is taken as 0.3, aspect ratio (a/b) is varied as 0.5, 1, 1.5 and 2. The different taper ratios (δ_o) that are considered here are 0.1, 0.25, 0.5 and 0.75. For practical purposes the thickness ratio is considered as h/a=0.001 (Table 2) and h/a=0.01 (Table 3). The first six non-dimensional parameters $\lambda = \omega a^2\sqrt{\rho h/D}$ obtained by the present formulation and program and are compared to available literature whenever possible and presented here. The Eigenfrequencies in Table 2 for h/a=0.001 is presented as new results. As expected there is negligible variation in calculated frequencies with rotary inertia and without rotary inertia for thin plates (Fig. 3). It is observed that the Eigenfrequencies increase with increase in the aspect ratio (a/b). When the taper ratio is increased the Eigenfrequencies increases. From Fig. 4 it might be concluded that rotary inertia has the effect of decreasing the frequencies. When rotary inertia is omitted it leads to over estimation of frequencies.

Table 5 Dimensionless frequencies $\lambda = \omega a^2\sqrt{\rho h/D}$ for skew SSSS taper rectangular plate

h/a	a/b	δ_o	α	Source	Modes					
					1	2	3	4	5	6
0.01	0.5	0.25	15	LSWRI(18X18)	20.9284	27.4522	39.716	57.2515	59.3501	66.0717
			30	LSWRI(18X18)	29.2637	34.9465	46.0746	62.5945	79.285	81.4232
			45	LSWRI(18X18)	41.3687	46.4269	56.6009	72.0632	91.1691	110.0784
		0.5	15	LSWRI(18X18)	22.7698	30.0792	43.6971	62.9276	65.0257	72.4428
			30	LSWRI(18X18)	32.0265	38.3421	50.6737	68.8899	86.8532	89.4697
			45	LSWRI(18X18)	45.4468	51.0445	62.31	79.3709	100.373	121.0543
	1	0.25	15	LSWRI(18X18)	27.6184	57.2804	68.0669	92.5242	117.5583	127.9561
			30	LSWRI(18X18)	35.4543	64.0809	89.3222	99.6487	137.6249	142.5196
			45	LSWRI(18X18)	47.3411	76.7983	112.8515	123.9018	153.5693	178.0527
		0.5	15	LSWRI(18X18)	30.265	63.0021	74.6879	101.8993	128.7461	140.4847
			30	LSWRI(18X18)	38.9037	70.4867	97.9985	109.6433	149.8282	158.2725
			45	LSWRI(18X18)	52.0368	84.5532	124.1555	136.2621	168.6524	196.2014
0.1	0.5	0.25	15	LSWRI(18X18)	15.1328	22.4789	34.4594	46.1359	50.3326	53.0054
			30	LSWRI(18X18)	20.0264	26.4195	37.3636	51.3423	56.5507	61.5489
			45	LSWRI(18X18)	29.2737	34.4447	43.9307	56.6106	70.1498	75.7137
		0.5	15	LSWRI(18X18)	16.5252	24.6123	37.5788	50.0002	54.5207	57.3588
			30	LSWRI(18X18)	21.6171	28.6752	40.538	55.433	60.7289	66.0966
			45	LSWRI(18X18)	31.3038	36.9872	47.2511	60.7323	74.9249	80.2608
	1	0.25	15	LSWRI(18X18)	22.6851	48.769	55.8953	75.5569	95.3249	99.1974
			30	LSWRI(18X18)	27.1649	51.6147	67.4317	76.825	104.1501	106.2431
			45	LSWRI(18X18)	35.8896	59.6322	83.1809	88.0821	108.5653	124.6347
		0.5	15	LSWRI(18X18)	24.8367	52.8514	60.4182	81.3011	101.6543	105.8044
			30	LSWRI(18X18)	29.4934	55.6755	72.3272	82.3864	109.9525	113.7296
			45	LSWRI(18X18)	38.5876	63.8239	88.3607	93.6748	114.6517	131.5005

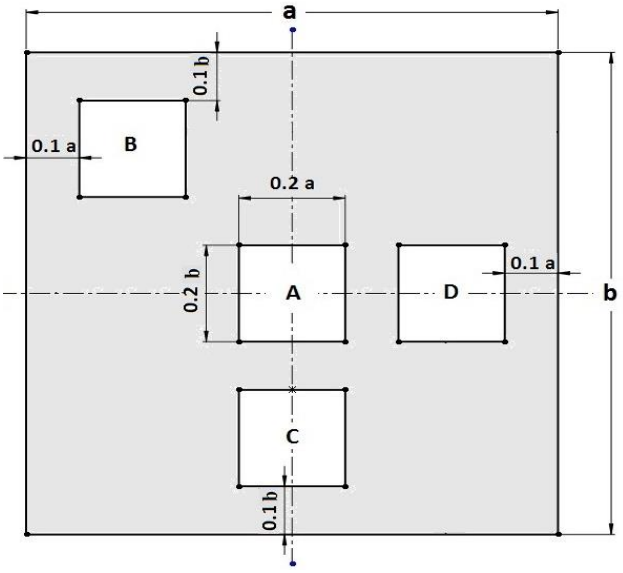

Fig. 5 Rectangular taper plate with internal rectangular cut-outs at various positions

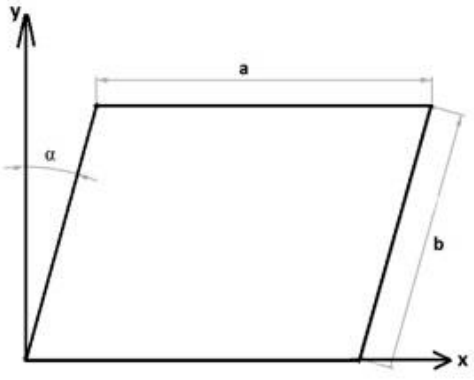

Fig. 6 Rectangular skew plate

4.2 Taper thickness rectangular plates with internal cutouts

Eigen frequencies for simply supported rectangular taper plates with internal cutouts at different locations (Fig. 5) are presented in this section. As shown in Fig. 5 four different positions of cutouts are selected for this study. A

Table 6 Dimensionless frequencies $\lambda = \omega a^2\sqrt{\rho h/D}$ for skew SSSS taper rectangular plate with central cutout

h/a	a/b	δ_o	α	Source	Modes					
					1	2	3	4	5	6
0.01	0.5	0.25	15	LSWRI(20*20)	20.618	27.193	40.12	50.55	56.298	64.464
			30	LSWRI(20*20)	29.058	34.65	46.701	60.255	63.402	81.011
			45	LSWRI(20*20)	40.663	45.96	57.162	69.791	75.232	92.131
		0.5	15	LSWRI(20*20)	22.444	29.778	44.066	55.427	61.947	70.686
			30	LSWRI(20*20)	31.803	38.005	51.189	66.193	69.998	88.839
			45	LSWRI(20*20)	44.55	50.536	62.451	76.707	83.612	101.594
	1	0.25	15	LSWRI(20*20)	27.21	55.486	64.214	90.654	114.816	129.731
			30	LSWRI(20*20)	34.956	62.073	80.292	99.211	133.15	139.597
			45	LSWRI(20*20)	45.889	73.9	99.426	113.402	150.894	168.362
		0.5	15	LSWRI(20*20)	29.858	60.996	70.398	99.87	125.697	140.994
			30	LSWRI(20*20)	38.416	68.259	88.116	109.107	144.97	155.014
			45	LSWRI(20*20)	50.507	81.336	109.433	124.774	165.679	185.976
0.1	0.5	0.25	15	LSWRI(20*20)	14.206	22.047	34.487	37.611	48.448	51.497
			30	LSWRI(20*20)	19.108	25.92	37.409	42.26	50.289	59.69
			45	LSWRI(20*20)	28.077	33.731	43.866	49.161	55.54	69.425
		0.5	15	LSWRI(20*20)	15.537	24.108	37.44	40.738	52.44	55.738
			30	LSWRI(20*20)	20.616	28.099	40.358	45.439	54.294	64.032
			45	LSWRI(20*20)	29.943	36.184	46.688	52.669	59.59	73.945
	1	0.25	15	LSWRI(20*20)	21.917	46.439	50.742	74.052	92.062	100.912
			30	LSWRI(20*20)	26.109	49.445	57.522	76.399	100.022	102.537
			45	LSWRI(20*20)	33.917	56.754	66.26	83.425	106.025	114.847
		0.5	15	LSWRI(20*20)	24.054	50.232	54.666	79.661	98.173	106.384
			30	LSWRI(20*20)	28.392	53.276	61.482	81.85	105.67	109.514
			45	LSWRI(20*20)	36.493	60.708	70.157	88.721	111.896	121.147

rectangular plate of dimension $a\times b$ with each cutout $0.2a\times 0.2b$ is modeled. The plates are taper in the x-direction as shown in Fig. 1. Since it has already been shown in the preceding subsection that the mass is lumping scheme with rotary inertia is more efficient in solving thick and moderately thick plate vibration, henceforth only LSWRI lumping scheme has been considered in this study. Though a sufficient convergence is achieved with 18*18 mesh size, a 20*20 mesh has been used for studying plates with internal cutouts due to some limitations in modeling the cutout in the home made FORTRAN program.

4.3 Taper thickness skew rectangular plates

The natural frequencies for simply supported skew rectangular plates with thickness varying uniformly in X-direction are presented in Table 5. The dimensions of the skew plate are as shown in Fig. 6. Moderately thick plates (h/a=0.01) and thick plates (h/a=0.1) with aspect ratios (a/b) 0.5 and 1 are considered here. Two different taper ratios 0.25 and 0.5 are studied with a combination of three different skew angles 15°, 30°, and 45°. It is observed that the Eigenfrequencies increase with an increase in skew angle (α).

4.4 Taper thickness skew rectangular plates with central cutout

The natural frequencies in non-dimensional form for simply supported skew rectangular plates with thickness varying uniformly in X-direction and internal cutout located centrally are presented in Table 6. The configuration of the cutout is similar to position "A" showed in Fig. 5. Rectangular plates with h/a=0.01and h/a=0.1 with aspect ratios a/b=0.5 and 1 are considered here. Three different skew angles 15°, 30° and 45° and two taper ratios 0.25 and 0.5 are studied.

5. Conclusions

The following conclusions are drawn from this study of free vibration analysis of tapered isotropic plates by using first-order shear deformation theory:

- The developed formulation using 9-node isoparametric element was tested for thin to moderately thick plates. In all cases, the obtained results are in close approximation to published solutions.
- Two types of mass lumping schemes were developed:

LSWRI is recommended for both thick and thin plates, whereas LSWORI is useful only for thin plates.

• As the thickness ratio (h/a) of the plate increases, the frequency parameter decreases.

• For plates without cutouts as the aspect ratio (a/b) increases, the fundamental frequency increases.

• The natural frequency increases with increase in skew angle.

• The increase in taper ratio δ_o causes the natural frequency to increase.

Due to the inherent features of the current analytical solution, the present findings will be a useful benchmark for evaluating other analytical and numerical methods that will be developed by researchers in the future.

References

Aksu, G. and Al-Kaabi, S.A. (1987), "Free vibration analysis of Mindlin plates with linearly varying thickness", *J. Sound Vib.*, **119**(2), 189-205.

Algazin, S.D. (2010), "Numerical algorithms of classical mathematical physics", Dialog-MIFI, Moscow.

Bert, C.W. and Malik, M. (1996), "Free vibration analysis of tapered rectangular plates by differential quadrature method: a semi-analytical approach", *J. Sound Vib.*, **190**(1), 41-63.

Bhat, R.B., Laura, P.A., Gutierrez, R.G., Cortinez, V.H. and Sanzi, H.C. (1990), "Numerical experiments on the determination of natural frequencies of transverse vibrations of rectangular plates of non-uniform thickness", *J. Sound Vib.*, **138**(2), 205-219.

Chakraverty, S. (2008), *Vibration of plates*, CRC press.

Cheung, K.Y. and Zhou, D. (1999a), "The free vibrations of tapered rectangular plates using a new set of beam functions with the Rayleigh-Ritz method", *J. Sound Vib.*, **223**(5), 703-722.

Cheung, Y.K. and Ding, Z. (1999b), "Eigenfrequencies of tapered rectangular plates with intermediate line supports", *Int. J. Solids Struct.*, **36**(1), 143-166.

Cheung, Y.K. and Zhou, D. (2003), "Vibration of tapered Mindlin plates in terms of static Timoshenko beam functions", *J. Sound Vib.*, **260**(4), 693-709.

Dalir, M.A. and Shooshtari, A. (2015), "Exact mathematical solution for free vibration of thick laminated plates", *Struct. Eng. Mech.*, **56**(5), 835-854.

Fantuzzi, N., Bacciocchi, M., Tornabene, F., Viola, E. and Ferreira, A.J. (2015), "Radial basis functions based on differential quadrature method for the free vibration analysis of laminated composite arbitrarily shaped plates", *Compos. Part B-Eng.*, **78**, 65-78.

Jin, G., Ye, T., Jia, X. and Gao, S. (2014), "A general Fourier solution for the vibration analysis of composite laminated structure elements of revolution with general elastic restraints", *Compos. Struct.*, **109**, 150-168.

Kalita, K. and Haldar, S. (2015), "Parametric study on thick plate vibration using FSDT", *Mech. Mechanic. Eng.*, **19**(2), 81-90.

Kalita, K. and Haldar, S. (2016), "Free vibration analysis of rectangular plates with central cutout", *Cogent Eng.*, **3**(1), 1163781.

Kandelousi, M.S. (2014), "Effect of spatially variable magnetic field on ferrofluid flow and heat transfer considering constant heat flux boundary condition", *Eur. Phys. J. Plus*, **129**(11), 1-12.

Kirchhoff, G. (1850), "Ueber die Schwingungen einer kreisf\"ormigen elastischen Scheibe", *Annalen der Physik*, **157**(10), 258-264.

Kirchhoff, G.R. (1850), *Uber das Gleichgewicht und die Bewegung einer elastischen Scheibe*.

Larrondo, H.A., Avalos, D.R., Laura, P.A. and Rossi, R.E. (2001), "Vibrations of simply supported rectangular plates with varying thickness and same aspect ratio cutouts", *J. Sound Vib.*, **244**(4), 738-745.

Lee, W.M. and Chen, J.T. (2010), "Scattering of flexural wave in a thin plate with multiple circular holes by using the multipole Trefftz method", *Int. J. Solids Struct.*, **47**(9), 1118-1129.

Lee, W.M., Chen, J.T. and Lee, Y.T. (2007), "Free vibration analysis of circular plates with multiple circular holes using indirect BIEMs", *J. Sound Vib.*, **304**(3), 811-830.

Liew, K.M., Xiang, Y. and Kitipornchai, S. (1995), "Research on thick plate vibration: a literature survey", *J. Sound Vib.*, **180**(1), 163-176.

Majumdar, A., Manna, M.C. and Haldar, S. (2010), "Bending of skewed cylindrical shell panels", *Int. J. Comput. Appl.*, **1**(8), 89-93.

Manna, M.C. (2006), "A sub-parametric shear deformable element for free vibration analysis of thick/thin rectangular plates with tapered thickness", *Appl. Mech. Eng.*, **11**(4), 901.

Manna, M.C. (2011), "Free vibration of tapered isotropic rectangular plates", *J. Vib. Control*, **18**(1), 76-91.

Mindlin, R.D. (1951), "Influence of rotary inertia and shear on flexural motions of isotropic elastic plates".

Mlzusawa, T. (1993), "Vibration of rectangular Mindlin plates with tapered thickness by the spline strip method", *Comput. Struct.*, **46**(3), 451-463.

Ozdemir, Y.I. and Ayvaz, Y. (2014), "Is it shear locking or mesh refinement problem?", *Struct. Eng. Mech.*, **50**(2), 181-199.

Pachenari, Z. and Attarnejad, R. (2014), "Analysis of Tapered Thin Plates Using Basic Displacement Functions", *Arab J. Sci. Eng.*, **39**(12), 8691-8708.

Pachenari, Z. and Attarnejad, R. (2014), "Free vibration of tapered mindlin plates using basic displacement functions", *Arab J. Sci. Eng.*, **39**(6), 4433-4449.

Pandit, M.K., Haldar, S. and Mukhopadhyay, M. (2007), "Free vibration analysis of laminated composite rectangular plate using finite element method", *J. Reinf. Plast. Comp.*, **26**(1), 69-80.

Rajasekaran, S. and Wilson, A.J. (2013), "Buckling and vibration of rectangular plates of variable thickness with different end conditions by finite difference technique", *Struct. Eng. Mech.*, **46**(2), 269-294.

Reddy, J.N. (1984), "A simple higher-order theory for laminated composite plates", *J. Appl. Mech.*, **51**(4), 745-752.

Reissner, E. (1944), "On the theory of bending of elastic plates", *J. Math. Phys. Camb.*, **23**(1), 184-191.

Reissner, E. (1945), "The effect of transverse shear deformation on the bending of elastic plates".

Saeedi, K., Leo, A., Bhat, R.B. and Stiharu, I. (2012), "Vibration of circular plate with multiple eccentric circular perforations by the Rayleigh-Ritz method", *J. Mech. Sci. Technol.*, **26**(5), 1439-1448.

Sahoo, S. (2015), "Laminated composite stiffened cylindrical shell panels with cutouts under free vibration", *Int. J. Manufact. Mater., Mech. Eng. (IJMMME)*, **5**(3), 37-63.

Viola, E., Tornabene, F. and Fantuzzi, N. (2013), "General higher-order shear deformation theories for the free vibration analysis of completely doubly-curved laminated shells and panels", *Compos. Struct.*, **95**, 639-666.

Ye, T., Jin, G., Chen, Y., Ma, X. and Su, Z. (2013), "Free vibration analysis of laminated composite shallow shells with general elastic boundaries", *Compos. Struct.*, **106**, 470-490.

Ye, T., Jin, G., Su, Z. and Chen, Y. (2014), "A modified Fourier solution for vibration analysis of moderately thick laminated plates with general boundary restraints and internal line supports", *Int. J. Mech. Sci.*, **80**, 29-46.

Zhou, D. (2002), "Vibrations of point-supported rectangular plates

with variable thickness using a set of static tapered beam functions", *Int. J. Mech. Sci*., **44**(1), 149-164.

CC

Symbols

[B]	Strain displacement matrix
[D]	Rigidity matrix
[K]	Global stiffness matrix
[N]	Shape function
$[N_0]$	Null matrix
$[M]$	Consistent mass matrix
$\|J\|$	Jacobian matrix
$[N_r]$	Interpolation function of the r^{th} point
$[K_0]$	Overall stiffness matrix
$[M_0]$	Overall Mass matrix
w	Transverse displacement
θ_x θ_y	Total rotations in bending
E	Modulus of elasticity
G	Modulus of rigidity
ν	Poisson's ratio
h	Thickness of plate
a, b	Plate dimensions
D	Flexural rigidity
ω	Natural frequency
$\phi_x \phi_y$	Average shear rotation
θ_x θ_y	Total rotation in bending
$\{\sigma\}$	Stress vector
$\{\varepsilon\}$	Strain vector
M_x, M_y	Bending moments in x and y direction
M_{xy}	Twisting moment
Q_x Q_y	Transverse shear forces
ξ, η	Natural coordinates
ρ	Density